ACS OMEGA

http://pubs.acs.org/journal/acsodf

Article

Improvement of In Vitro Dissolution of the Poor Water-Soluble Amlodipine Drug by Solid Dispersion with Irradiated Polyvinylpyrrolidone

Mohamed Mohamady Ghobashy,* Dalal Mohamed Alshangiti, Sheikha A. Alkhursani, Samera Ali Al-Gahtany, Fathiah Salem Shokr, and Mohamed Madani*

Cite This: *ACS Omega* 2020, 5, 21476−21487

Read Online

ACCESS | Metrics & More | Article Recommendations

ABSTRACT: The aim of this study was to increase both the rates of dissolution and bioavailability of the amlodipine (Amlo) drug. Due to the low cost, high solubility, and amorphous state, polyvinylpyrrolidone (PVP) has been used as a drug carrier in the solid dispersion process. Through applying an irradiation technique, powder of (PVP) is irradiated with six 0−50 kGy irradiation doses. The six irradiated (PVP) samples were characterized using gel permeation chromatography, electron spin resonance, and Fourier transform infrared (FT-IR) spectroscopy. The formulation of six (PVP/Amlo) samples at a ratio of 2:1 wt/wt were characterized using FT-IR spectroscopy and X-ray powder diffraction. In vitro dissolution of (Amlo) drug was assessed in a water solvent at pH 1.2 and pH 7. Results demonstrated that there is a change in the physicochemical properties of irradiated (PVP). FT-IR confirmed that there is an intermolecular H bond between the (Amlo) drug and (PVP) polymer. XRD confirmed that (PVP) changes the crystalline (Amlo) to amorphous amlodipine. Irradiated (PVP) at a dose of 20 kGy released approximately 89% from 40 mg of (Amlo) in 60 s. The in vitro rate of amlodipine dissolution depends on the drug−polymer intermolecular H bond. The rate of (Amlo) dissolution is increased due to the drug−drug intramolecular hydrogen bonding replaced with the drug−polymer intermolecular hydrogen bonding, which reduces the crystal packing. Irradiated (PVP) improved the rate of (Amlo) dissolution compared to unirradiated (PVP).

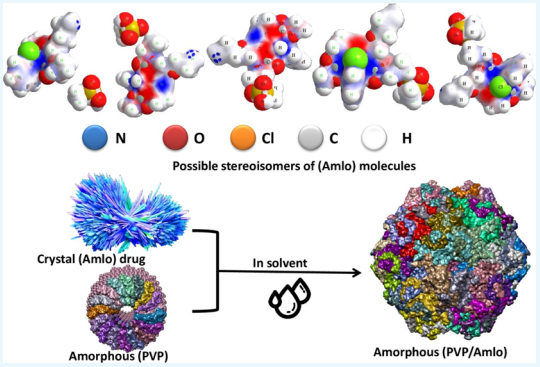

1. INTRODUCTION

Improving the bioavailability of insoluble drugs is one of the biggest problems, which is why several research papers were addressed.[1,2] The bioavailability and solubility of insoluble drugs have been improved by a solid dispersion method.[3−5]

Chiou and Riegelman[6] described solid dispersion as a binary system consisting of two substances, a hydrophilic polymer and a drug substance with hydrophobia. Polyvinylpyrrolidone (PVP) is used in this article because of its low cost, high water solubility, and amorphous structure form. Drugs tend to be more soluble under amorphous conditions than crystalline conditions.[7] This is because no energy is needed during dissolution of the amorphous lattice.[8] In most cases, very reactive intermediates are formed by subjecting the polymeric materials in a solid state to ionizing radiation (gamma rays, X-rays, accelerated electrons, ion beam), which leads to changes in their physiochemical properties.[9,10] Based on the polymer's composition, various polymers have different effects of radiation. Various studies on the impact of ionizing radiation on polymeric materials show several structural changes in their macromolecular structure.[11−13] These include the removal of atoms, carbonization, and the production of free radicals,[14] which may cause scission or cross-linking processes.[15] Both processes are dependent on the polymer's nature and the atmospheric conditions.[16−18] It concludes that the scission cross-linking are a competing phenomenon.[19] Polymer irradiation is somewhat different in aqueous solutions than solids or in pure monomers.[20,21] Gamma irradiation-driven ring opening of polymer cycles in the absence of oxygen,[22] like in (PVP),[23] gives free functional groups that may undergo hydrogen-bonding interactions.[24−26] It is a complex phenomenon,[27] which involves a combination of scission-cross-linked processes. As an excipient, (PVP) is widely used, particularly in solutions and oral tablets because of its ability to dissolve in oil and water.

Received: April 30, 2020
Accepted: July 8, 2020
Published: August 18, 2020

https://dx.doi.org/10.1021/acsomega.0c01910
ACS Omega 2020, 5, 21476−21487

This research aims to establish an improvement of amlodipine solubility that could be used to treat chronic stable angina, hypertension, and confirmed or suspected angina. Amlodipine is a slow-channel blocker or a calcium ion antagonist that prevents calcium ion on the transmembrane into the heart and vascular smooth muscle. Amlodipine besilate is known as slightly soluble in water and is described as an ionized compound (weak base); pKa is 8.6 at 25 °C.

Yu et al.[28] investigated the important of calcium channel blockers in diabetes treatment. CaV3.1 channels become hyperactive along with the occurrence of diabetes. This leads to a reduced insulin-secretion capacity of β-cells and aberrant glucose homeostasis. The researchers evaluated the high expression of the β-cell. The CaV3.1 channel impairs insulin release and homeostasis of glucose. This confirms the importance of the amlodipine drug for treating many diseases.

Different excipients are reported for enhancement the solubility and dissolution of the amlodipine drug (Amlo) and its therapeutic efficacy. The solid dispersions of the amlodipine drug (Amlo) was prepared through a solid dispersion method using varying concentrations of excipients such as crospovidone,[29] croscarmellose sodium, sodium starch glycolate,[30] polyethylene glycol (PEG),[31−33] and starches with hydroxypropyl methyl cellulose.[34]

Jang et al.[35] used the solid dispersion method to disperse the amlodipine drug (Amlo) in large amounts with dextrin (Amlo/SD) (1:10 wt/wt) in the existence of an absorption enhancer such as SLS (0.9% w/w). The comparative in vitro dissolution study of (Amlo-SD) and (Amlo) was carried out at pH 1.2 and pH 6.8. It was found that 86% of the amlodipine drug (Amlo) was dissolved from (Amlo−SD) formulation after 10 min at pH 1.2 compared with 31% of the blank sample. Also in pH 6.8, the dissolution of the amlodipine drug (Amlo) from (Amlo−SD) was higher than that from the blank sample.

Pare et al.[36] prepared different floating effervescent tablets of the amlodipine drug (Amlo) and analyzed their various physicochemical characteristics such as releasing the drug from its active ingredient. Various hydrophilic and hydrophobic polymers such as hydroxypropyl methylcellulose and Carbopol 934P with sodium bicarbonate and citric acid as effervescent agents were mixed with the amlodipine drug (Amlo). The developed tablets were compared to the conventional formulations, and it was found that their release was delayed twice (24 h) compared to that of the products on the market (12 h).

Shelke et al.[37] prepared a film that consists of the Amlodipine drug (Amlo) and sodium alginate as the drug carrier and sodium starch glycolate as the drug disintegrant in nine various concentrations through the solvent casting technique. The in vitro dissolution study was carried out at pH 6.2, and it was observed that almost 75−80% of the amlodipine drug (Amlo) was released after 6 min in all the formulations.

The irradiated (PVP) polymer and amlodipine drug (Amlo) interactions have been performed based on experimental FT-IR and XRD data. Polyvinylpyrrolidone (PVP) powder was irradiated by applying gamma rays at different doses (0, 10, 20, 30, 40, and 50 kGy) in order to obtain (PVP) of different molecular weights. The influence of gamma radiation on the change of the molecular weight and chemical structure has been investigated.

2. EXPERIMENTAL SECTION

2.1. Materials. A water-soluble polymer, polyvinylpyrrolidone (PVP) with an average molecular weight (*M*w) of 100 kDa (highly viscous), was purchased from Sigma-Aldrich Co. Amlodipine besilate was received as a gift sample from Nile Pharmaceuticals, Cairo, Egypt (Scheme 1).

Scheme 1. Chemical Structure of Polyvinylpyrrolidone and Amlodipine Besilate

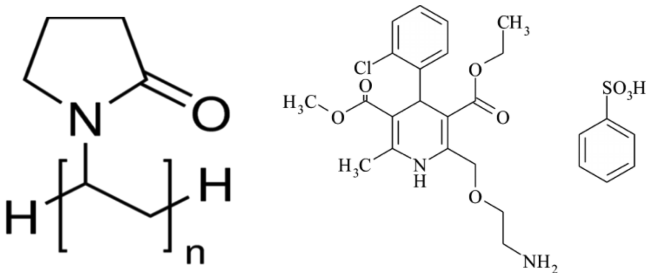

2.2. Gamma Irradiation of Solid (PVP) Powder. (PVP) powder was exposed, in closed vessels filled with N_2 gas, to ^{60}Co gamma radiation and purged with nitrogen gas to prevent radiation−oxidation of (PVP). The five implemented radiation doses are 10, 20, 30, 40, and 50 kGy performed at a dose rate of 2.08 kGy/h. The irradiated samples were kept in a closed vial until examined through analytical characterization.

2.3. Preparation of Amlodipine Dispersions in Irradiated (PVP) by the Solid Dispersion Technique. Solid dispersions of amlodipine in combination with a (PVP) blank and with irradiated (PVP) at doses of 10, 20, 30, 40, and 50 kGy were prepared. Briefly, in a conventional solvent evaporation method, 0.5 g of amlodipine and 1 g of each of six irradiated (PVP) powder samples were dissolved in 20 mL of ethanol. We maintained a 2:1 w/w polymer/drug ratio to optimize the (PVP) space in which amlodipine is to be distributed to ensure that the drug is well linked to the polymer matrix that can effectively dissolve the drug. The six solutions of amlodipine−(PVP) were dried under vacuum. The resultant six samples of drug−polymer in solid dispersion (Table 1) are pulverized in a mortar and pestle.

Table 1. Experimental Procedures of the (PVP) Processing by Gamma Radiation Technique

	first step (PVP, dried solid sample)	second step	
product sample	radiation dose (kGy)	mix (PVP/AMLO) (wt/wt)	product sample
(S-0)	0	1/0.5	(PA-0)
(S-10)	10	1/0.5	(PA-10)
(S-20)	20	1/0.5	(PA-20)
(S-30)	30	1/0.5	(PA-30)
(S-40)	40	1/0.5	(PA-40)
(S-50)	50	1/0.5	(PA-50)

2.4. Measurement of the In Vitro Dissolution Profile. The release rate of (Amlo) from the (PVP/Amlo) was measured from dissolution of 120 mg of (PVP/Amlo) in 100 mL of water solution in both pH 7 and pH 1.2 every 60 s; samples of 3 mL were withdrawn from the solution and assayed spectrophotometrically for the drug.

https://dx.doi.org/10.1021/acsomega.0c01910
ACS Omega 2020, 5, 21476−21487

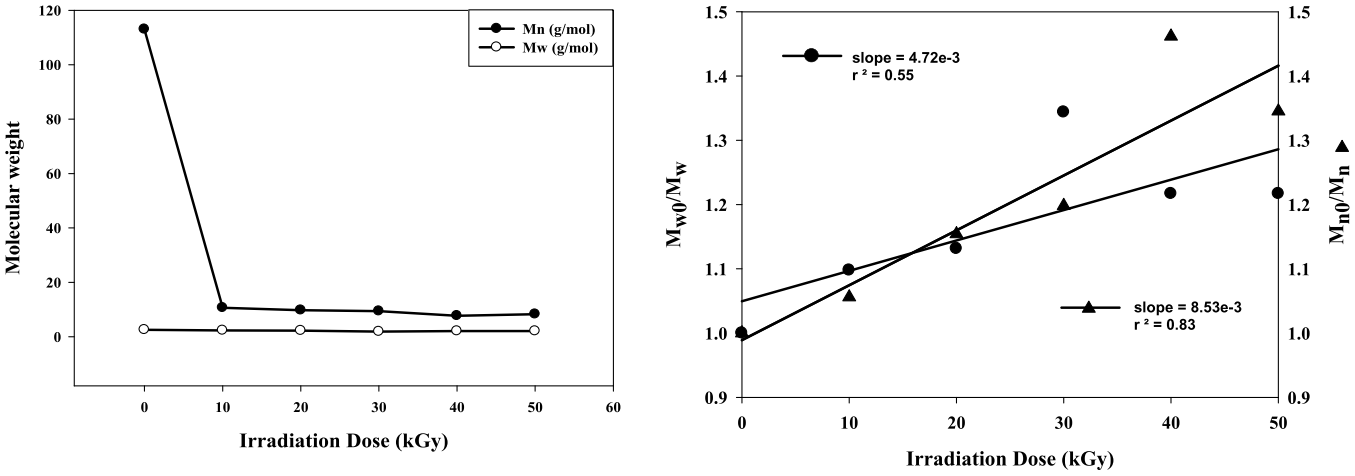

(a) (b)

Figure 1. (a) Variation of weight average (M_w) and number average (M_n) of the molecular weight as a function of the irradiation dose. (b) Graphical determination of τ for irradiated (PVP).

2.5. Characterization. *2.5.1. X-Ray Diffraction.* An X-ray diffraction pattern was used to measure the effect of irradiated (PVP) on the crystallinity of solid (Amlo) samples. The model of the X-ray diffraction patterns is XRD-6000 series. A solid (PVP) polymer, (Amlo) drug, and corresponding physical mixtures of (PVP/Amlo) samples were analyzed via an X-ray diffraction apparatus using a nickel filter with a scan speed = 8 deg/min, Cu K target, current = 30 mA, and voltage = 40 kV from the Shimadzu company Shimadzu Scientific Instruments (SSI), Kyoto, Japan.

2.5.2. Fourier-Transforms Infrared Spectra (FT-IR). FT-IR records were conducted with a Mattson 1000 Unicom, England, spectrometer within the wavenumber range 500−4000 cm^{-1}.

2.5.3. Electron Spin Resonance (ESR). ESR was performed post-irradiation storage on the solid (PVP). The five irradiated samples of (PVP) from 10 up to 50 kGy along with blank samples of solid (PVP) (0 kGy) are irradiated again at 20 kGy in air atmosphere. The samples were measured immediately after irradiation took place. A Bruker EMX spectrometer (X-band) device from Bruker, Germany, was used to monitor ESR signals at room temperature.

2.5.4. GPC Measurements. The molecular weights of the irradiated solid (PVP) powder were determined by gel permeation chromatography (GPC) with an alginate GPC system equipped with a calibrated refractive-index detector (RID A). The eluent used was a water aqueous solution sonicated at a 0.5 mL/min flow rate.

2.5.5. Scanning Electron Microscopy (SEM). The grain morphology and the crystalline of irradiated (PVP) and (Amlo) powders were obtained using scanning electron microscopy (SEM) with the working operation at 20 kV (JEOL JSM-5400, Jeol Ltd., Tokyo, Japan). All samples were coated with a thin layer of gold. Images of these samples were taken using an optical microscope with 150, 1500, and 2000× magnifications.

3. RESULTS AND DISCUSSIONS

3.1. Gamma Irradiation-Induced Ring Opening of the Pyrrolidone Molecule. As known, gamma ray irradiation greatly affects the chemical structure of polymeric materials due to the simultaneous cross-linkage and scission processes.[38,39] As expected, the effect of gamma irradiation on the polymer sample of (PVP) powder is subjected to inert gas (N_2), which promotes the scission reactions compared to cross-linkage reactions.[40] This was reflected in the changes in their physicochemical properties.

Table 2. Data Extracted from GPC and Radiation Chemical Yield of Scission (G_s) of Solid Irradiated (PVP)

irradiation dose (kGy)	M_n (g/mol) 10^5	M_w (g/mol) 10^5	M_z (g/mol) 10^5	PDI	G_s	conversion (%)
S-0	1.13	2.58	5.73	2.28		97.82
S-10	1.07	2.35	5.34	2.19	0.88268	84.78
S-20	0. 979	2.28	5.18	2.33	0.648487	92.59
S-30	0.943	1.92	3.80	2.03	1.172565	91.46
S-40	0.773	2.12	5.25	2.74	0.677189	99.04
S-50	0.84	2.12	5.16	2.52	0.49854	98.07

3.1.1. GPC, ESR, and FT-IR Study of the Altered Physicochemical Properties of Irradiated (PVP) Powder. Figure 1a exhibits a systematic decrease in weight (M_w), number (M_n), and average molecular weight as a result of an irradiation dose through the formation of polymer species of lower molecular weight. The quantitative characterization of the radiation degradation of polymers in terms of scission and cross-linking was done. To quantify radiation chemical scission yields, G_S, and cross-linking G_X for (PVP) solid powder. These two parameters are defined by the relationships

$$G_s = 9.65 \times 10^9 \tau / M_1 \quad (1)$$

$$G_x = 9.65 \times 10^9 \chi / M_1 \quad (2)$$

where M_1 is the monomer molecular weight, τ and χ are the probabilities of scission and cross-linking, respectively.

Charlesby[41] and Saito and Osamu[42] developed the scission and cross-linking theory of the chains of the polymer by statistical calculation using the following assumptions:

1. All polymers should be linear.
2. G_s and G_x are dose independent.
3. Although the cross-linking and scission processes occur simultaneously, it is assumed that independence of the two cross-linking and scission phenomena is to be treated consecutively.

https://dx.doi.org/10.1021/acsomega.0c01910
ACS Omega 2020, 5, 21476−21487

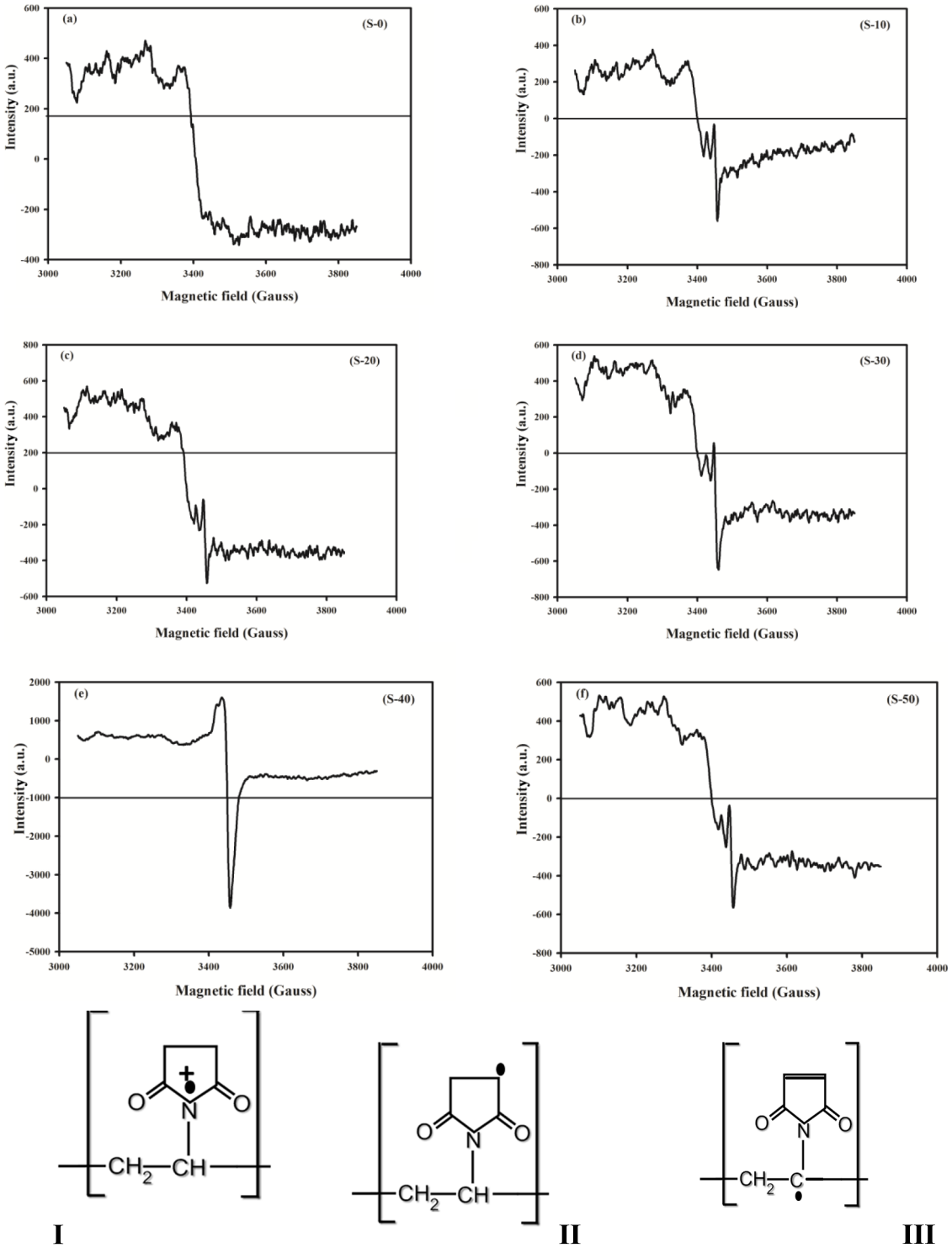

Figure 2. First derivative of the ESR spectrum of the post-irradiation (PVP) solid state initiated by ^{60}Co gamma radiation (20 kGy) at room temperature for (a) neat (PVP) and irradiated (PVP) at (b) 10, (c) 20, (d) 30, (e) 40, and (f) 50 kGy with respect to the applied magnetic field (Gauss). Below shows the pictures of the probability of where the unpaired electrons are centered.

4. All monomer units have the same probability of cross-linking or scission.
5. Neglect end group effects.

Graphical values of τ and χ were obtained from the following eqs 3 and 4:

$$\frac{M_n(0)}{M_n(D)} = 1 + \mu(\tau - \chi)D \quad (3)$$

$$\frac{M_w(0)}{M_w(D)} = 1 + \mu(\tau - 4\chi)D \quad (4)$$

with the initial average number molecular weight denoted as $M_n(0)$, after radiation dose denoted as D, and average number molecular weight denoted as $M_n(D)$. In the same way, the initial average molecular weight is denoted as $M_w(0)$, after irradiation

https://dx.doi.org/10.1021/acsomega.0c01910
ACS Omega 2020, 5, 21476−21487

Table 3. ESR Parameters of the Post-irradiation (PVP) Solid State Initiated by Gamma Radiation (20 kGy)

product sample	g//	g⊥	Hr(Oe)	ΔH
(S-0)				
(S-10)	2.00937	2.01211	3452.73	9.9
(S-20)	2.00943	2.01217	3452.73	10.89
(S-30)	2.00934	2.01253	3452.73	12.87
(S-40)	2.01068	2.01935	3450.39	23.77
(S-50)	2.00937	2.01211	3452.73	9.9

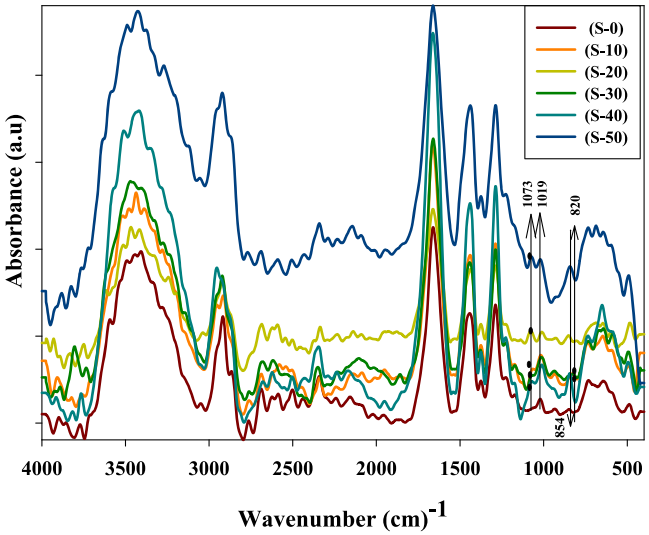

Figure 3. FT-IR spectra of irradiated solid (PVP) up to 50 kGy.

Scheme 2. Proposed Scission Mechanism for the Impact of Gamma Irradiation on Solid (PVP) Causing the Ring Opening of the Pyrrolidone Ring at a Nitrogen Atmosphere

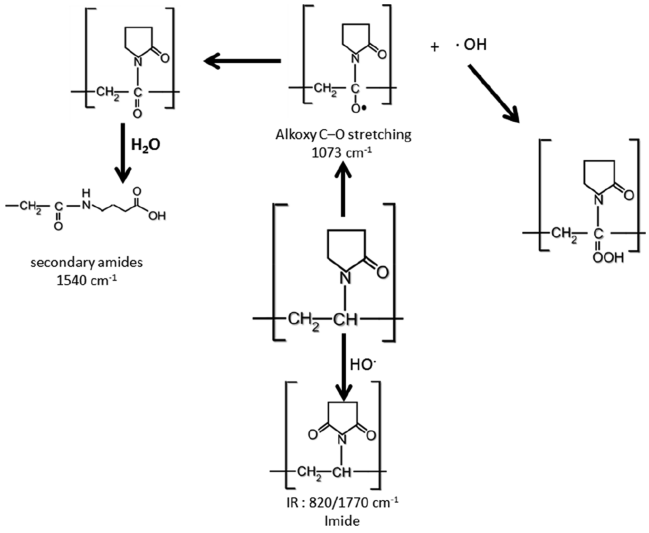

dose is denoted as D, and average molecular weight denoted as $M_w(D)$. The average number of monomer unit is μ.

By assuming that the scission effect is the major effect of irradiation and no crosslinking occurred during irradiation process, the value of $G_x = 0$. Consequently, by replacing $\chi = 0$ in eqs 3 and 4, the following are obtained:

$$\frac{M_n(0)}{M_n(D)} = 1 + \mu\tau D \quad (5)$$

$$\frac{M_w(0)}{M_w(D)} = 1 + \mu\tau D \quad (6)$$

From the slope of Figure 1b, it could be possible to calculate the τ value. Using the graphical determination of τ, it possible to calculate G_s (Table 2). As seen in Table 2, the chemical yield of scission G_s is slightly affected by the gamma irradiation dose. At an irradiation dose of 30 kGy, the G_s of (PVP) was the largest and returned to a decrease at irradiation doses of 40 and 50 kGy. This could due to the cross-linked reaction that took place, which was confirmed by increased PDI values to 2.74 and 2.52 for 40 and 50 kGy, respectively. These results confirmed that the gamma irradiation may have caused the decrease in G_s and increased in PDI that are in agreement.[43,44]

The electron spin resonance (ESR) technique is a direct method to measure the chain scission.[45] Certainly, radiation-produced free radicals that have been accumulated were detected using the ESR instrument. The five irradiated solid (PVP) at 10−50 kGy belong to unirradiated samples (S-0) were irradiated again at 20 kGy in air atmosphere. The samples were measured immediately after irradiation at room temperature to detect the radicals accumulated. The first derivative ESR spectrum of the (S-0) blank sample (neat PVP) was recorded as shown in Figure 2a; no hyperfine splitting was observed due to the high localization of the unpaired electron, which is mainly confined in a p orbital of a N atom in the pyrrolidone ring in a neutral state. The first-derivative curves (Figure 2b−f) show a signal of very low intensity ranging from 3000 to 3850 G with noise. This means that the radicals that prevail in the system are stable enough at room temperature. The shape of the spectrum (Figure 2) was a hyperfine interaction, which indicates the existence of the interaction of unpaired electrons of the nitrogen nucleus and free radicals in carbon positions of the pyrrolidone ring.[46,47] As shown in Figure 2b−f of radiation doses from 10 up to 50 kGy, there are anisotropic signals between $g//$ and $g\perp$ due to the existence of the hyperfine interaction. Figure 2b shows the asymmetric triplet-line spectrum for (S-10); the conclusion is that an unpaired electron interacts with one corresponding proton at the Cα atom of the polymer chain[48] or it could be attributed to proxy radicals.[49] In Figure 2c,d, no alteration of the triplet-line spectrum can be observed. Therefore, it can be concluded that the radicals localized at the Cα atom of the polymer chain. In Figure 2e for (S-40), the line spectrum was changed to a wide line like that obtained from poly(vinyl carbazole)[50] due to concerned radicals with an unpaired electron centered at the N atom (I). It could be confirmed that the radical was produced by C−H scission in the alkyl side chain of *N*-phenylmaleimide (II) where the radicals center at Cβ;[51] these radicals have total spectra width from (S-10 ,S-20 ,S-30, and S-50) of ΔH = 9.9, 10.89, 12.87, and 9.9, respectively, that is less than ΔH for radical (I) and radical (II) from (S-40) where ΔH = 23.77; this indicated that the cation radicals centered at the N atom and at Cβ associated with radicals at Cα, forming a double pond (III). Figure 2f shows a triplet-line spectrum due to richness of free radicals in case the (S-50) sample is similar to the line spectrum of (S-10, S-20, and S-30). There was a predominance of the triplet to the propagating radical (II) and (III). The integrated intensity of the spectrum is proportional to the concentration of radicals in the sample (Table 3); the intensity of the peak at (S-40) is highly indicative of the increase in the stability of radicals formed rather than increase in the number of radicals.

https://dx.doi.org/10.1021/acsomega.0c01910
ACS Omega 2020, 5, 21476−21487

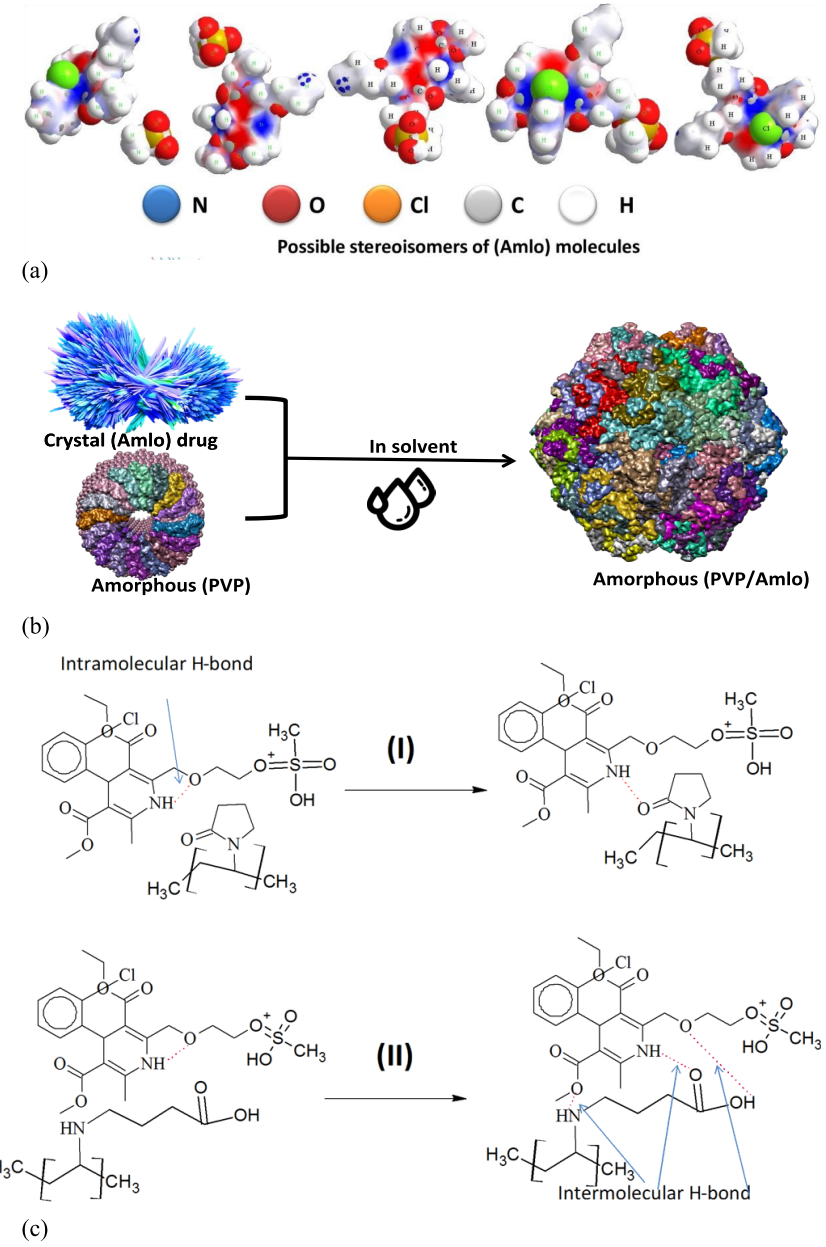

Figure 4. Outline of (a) hydrophilic and hydrophobic sides of the amlodipine besilate drug. (b) Amorphous solid dispersion. (c) Proposed mechanism of formation of drug−drug and drug−polymer intramolecular and intermolecular hydrogen bonding, respectively. H bonds are shown as red lines.

FT-IR-ATR spectroscopy was used to assess the structural changes in (PVP) polymers and their derivatives after their irradiation. FT-IR spectra of the non-irradiated and irradiated (PVP) powders at different doses are shown in Figure 3. The spectrum of the unirradiated sample (S-0) indicates the absorbance peak at 845 cm^{-1} corresponding to the characteristic (PVP) rings.[52] The peak at 1019 cm^{-1} represents the functional group C−N in (PVP) rings.[53]

The corresponding peak at 1660 cm^{-1} for the C═O bond in (PVP) rings becomes wider, and a shoulder with radiation dose increases; this means that the increase in the H bond involved pyrrolidone ring opening (see Scheme 2). In addition, broad peaks from 3060 to 3700 cm^{-1} for OH and NH groups are wider with the radiation dose rising up to 50 kGy as shown in Figure 3 . The absorbance peak at 820 cm^{-1} that is bound for the two samples (S-10) and (S-30) irradiated with 10 and 30 kGy was observed, respectively; and stingy in the other doses, the peak at 1770 cm^{-1} was observed for all radiation doses and pyrrolidone ring openings at different radiation doses, and this results in the formation of the imide groups (see Scheme 2). In the meantime, the peak at 1540 cm^{-1}, which increases after irradiation, can be attributed to the bending vibration of the secondary amide N−H bond,[54] whereby the peak at 1073 cm^{-1} is attributed to the alkoxy C−O group stretching[55] (see Scheme 2).

As an overall result, at higher doses, the radiolysis of (PVP) caused ring opening, the radical produced due to gamma irradiation has a high effect on changing the chemical structure of (PVP) molecules. This could reflect in using irradiated (PVP) in pharmaceutical applications; here, some of these applications have been performed. Amlodipine besilate (Amlo) is known as an insoluble drug. The purpose is to improve the rates of solubility and dissolution by cooperating with irradiated (PVP) powder by a solid dispersion technology.

https://dx.doi.org/10.1021/acsomega.0c01910
ACS Omega 2020, 5, 21476−21487

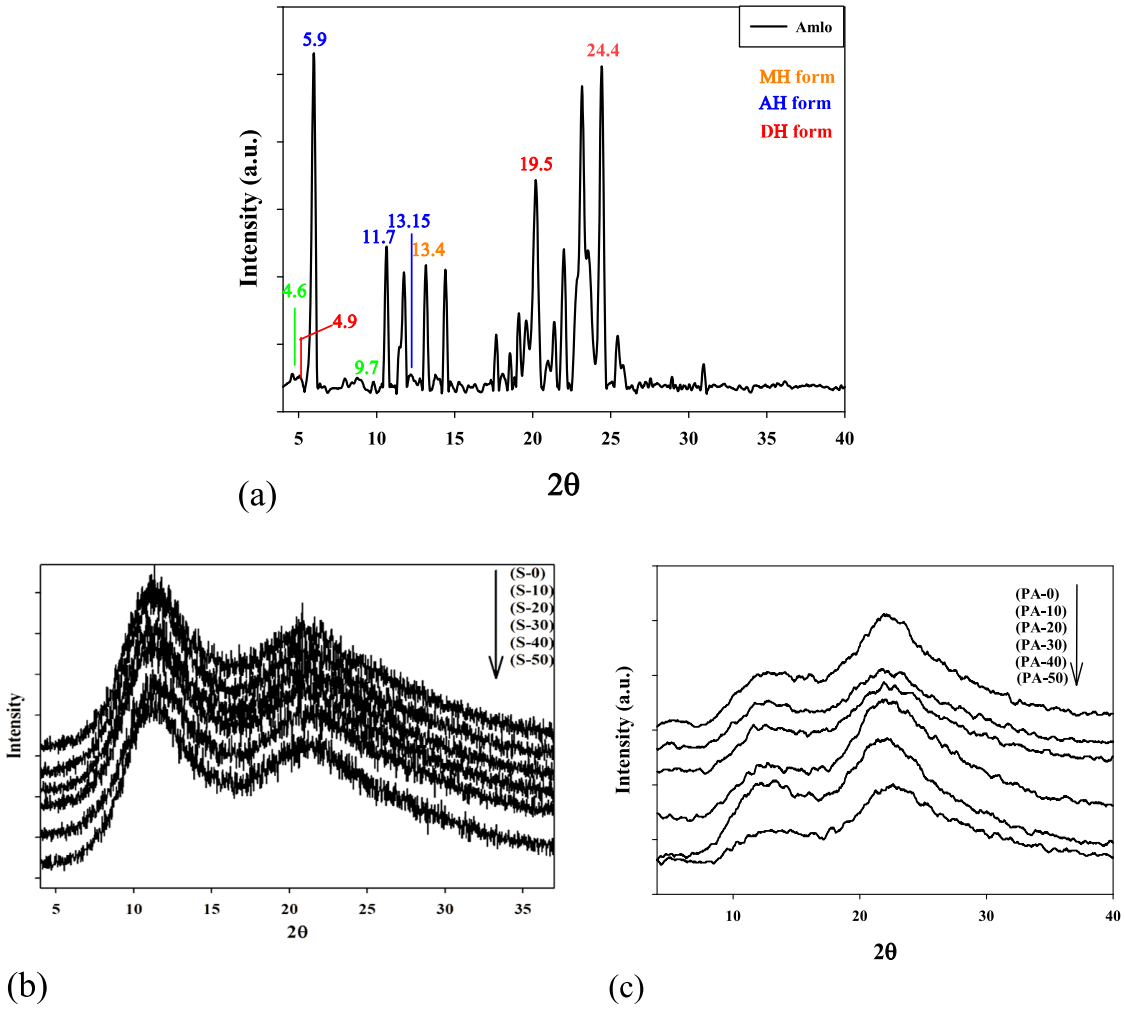

Figure 5. X-ray diffraction of (a) amlodipine besilate. Irradiating (b) solid (PVP) and (c) (PVP/Amlo) up to 50 kGy.

Table 4. Crystal Size (D, nm) of Irradiated (PVP) Powder

sample no.	I/I_o	2θ	FWHM (deg)	β rad	D (nm)
S-0	100	10.84	2.8339	0.049460886	2.815822656
S-10	100	10.84	3	0.052359878	2.662060916
S-20	100	11.1	3.6	0.062831853	2.218867477
S-30	100	11.34	7.79	0.135961149	1.025618281
S-40	100	11.34	8.79	0.153414441	0.908938158
S-50	100	10.74	8.98	0.156730567	0.889256637

3.2. Proposed Chemical Interaction of (PVP) and (Amlo) Molecules. The changes in the chemical structure of irradiated (PVP) molecules give different probabilities of interaction between (Amlo) drug molecules and irradiated (PVP) samples. The internal interaction between the (PVP) carrier and the drug leads to some differences in their solubility rate. The possibility of a chemical interaction between (Amlo) and (PVP) is outlined in Figure 4. In the AH form, the amlodipine molecules have one intramolecular H bond.[56] As known, the existence of intramolecular hydrogen bonds in drug molecules significantly reduced their solubility and bioavailability.[57] To enhance drug solubility as well as dissolution kinetics, the formation of intermolecular hydrogen bonding between drug molecules and hydrophilic carriers should be obtained.[58] Figure 4 underlines the drug−polymer molecular interactions that govern the properties of solid dispersions, and the research articles of understanding the drug-polymer interaction lack profoundness.[59]

Figure 4a shows the hydrophilic and hydrophobic sides of the amlodipine drug, the aromatic ring and chloride atom are considered as a hydrophobic region that would cause repelling of water molecules and currently reduced drug solubility. Only two sides (O and N atoms) in the (Amlo) structure are considered as a hydrophilic region and directly form hydrogen bonds with the (PVP) polymer. This finds a way for amorphous solid dispersion, thereby increasing the solubility of the drug and reducing the necessary dosage.

Figure 4b shows representation of the dissolution process for polymer−drug molecules. The structure form of (Amlo) drug is crystalline, where (Amlo−Amlo) interactions are strong enough due to intramolecular H bonds, and the solubility process happens slowly.

The polymer−solvent interactions are strong due to the amorphous structure form of the polymer, which plays a role in this case. It is desirable to start an interaction with the solvent that is strong enough in order to expose more of their area for unfolding polymer chains, hoping for disintegration of the amorphous state. Thus, the whole loosen coil will diffuse into the crystallite (Amlo) drug. Therefore, the (Amlo) drug is dispersing into a solution. At this stage, the disintegration of the crystalline structure by the interaction with (PVP) polymer increases the rate of drug dissolution.

https://dx.doi.org/10.1021/acsomega.0c01910
ACS Omega 2020, 5, 21476−21487

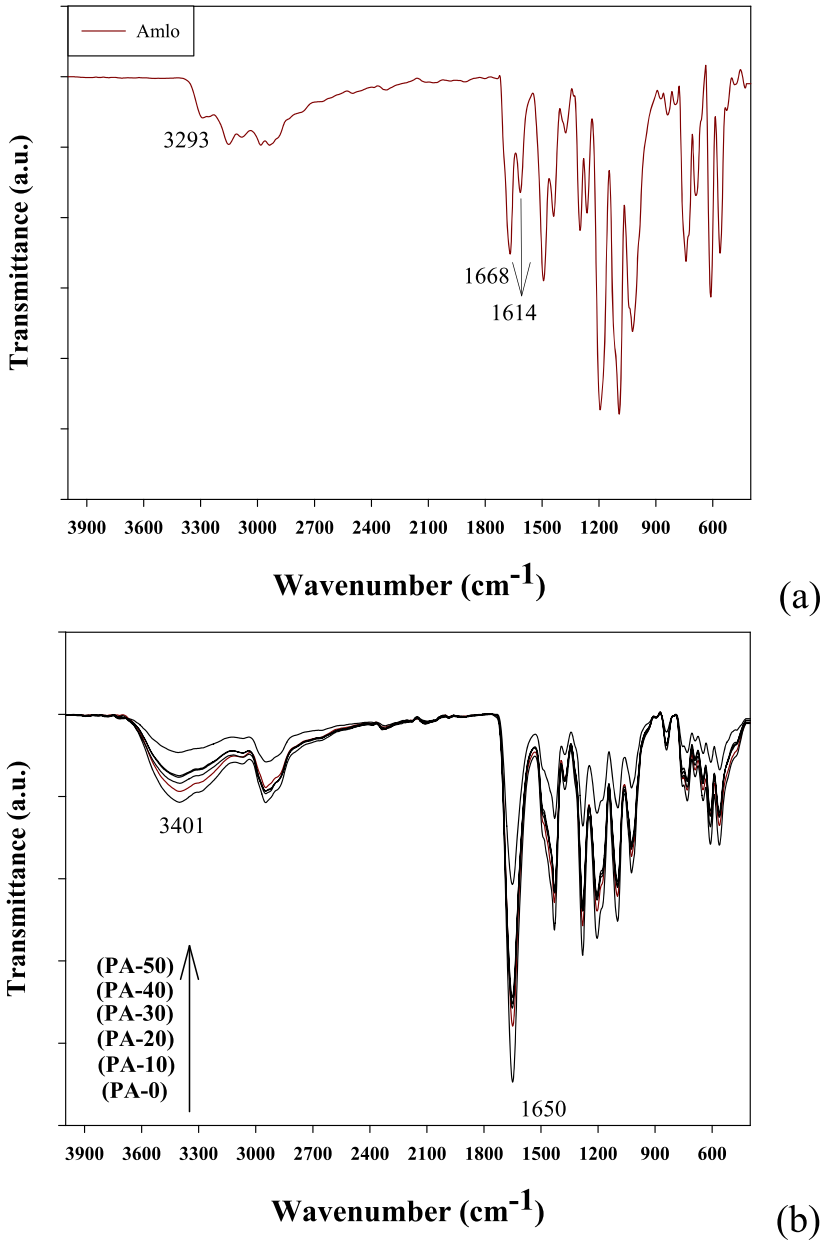

Figure 6. FT-IR of (a) (Amlo) and (b) (PVP/Amlo) samples.

The particular connotations such as the molecular weight and hydrophilic groups of (PVP) polymers are shown in Figure 4c, which explain how the polymer−drug intermolecular H-bond interaction is formed.

Case number (I) represented the interaction between the (Amlo) drug−drug interaction, which is intramolecular H bonds that are converted to intermolecular H bonds with unirradiated (PVP) polymers caused by the stability of the solid dispersion. Case number (II) represented the drug−polymer intermolecular hydrogen bonding using three hydrogen donor groups of the irradiated (PVP) molecule (opening PVP ring). The increased intermolecular hydrogen bonding is an effect on the crystal structure versus solid dispersion stability. In this conduct, the interaction of the (Amlo) drug with irradiated (PVP) is a more stable solid dispersion compared to that with unirradiated (PVP). This indicated that the opening (PVP) ring induced by gamma irradiation provides the stability of the dispersed (Amlo) drug molecules.

3.3. X-Ray Diffraction of Gamma-Irradiated Solid (PVP) and (PVP/Amlo). Figure 5a shows the XRD pattern of amlodipine besilate (Amlo), which exhibited the characteristic diffractions peaks of three solid forms of AML, indicating their distinct crystal structures. The XRD peaks located at 2θ = 5.9,11.7, and 13.15° corresponding to the (002), (004), and (023) plans were characteristic to AH, anhydrous form. The observed XRD diffraction peaks located at 2θ = 4.9, 13.4, 19.5, and 24.4° corresponding to the (100), (210), (400), and (222) planes were characteristic to DH, dehydrate form. Additionally, the diffraction XRD peaks for the MH, monohydrate form, were observed at 2θ = 4.6, 9.7, and 13.9°. The experimental XRD pattern of (Amlo) provides an excellent crystalline form that matches the AH, anhydrous form.

As shown in Figure 5b, the irradiated solid (PVP) gave a couple of broad bands located at 2θ = 11 and 22°. Those peaks are formulated with noise that could generally indicate the

https://dx.doi.org/10.1021/acsomega.0c01910
ACS Omega 2020, 5, 21476−21487

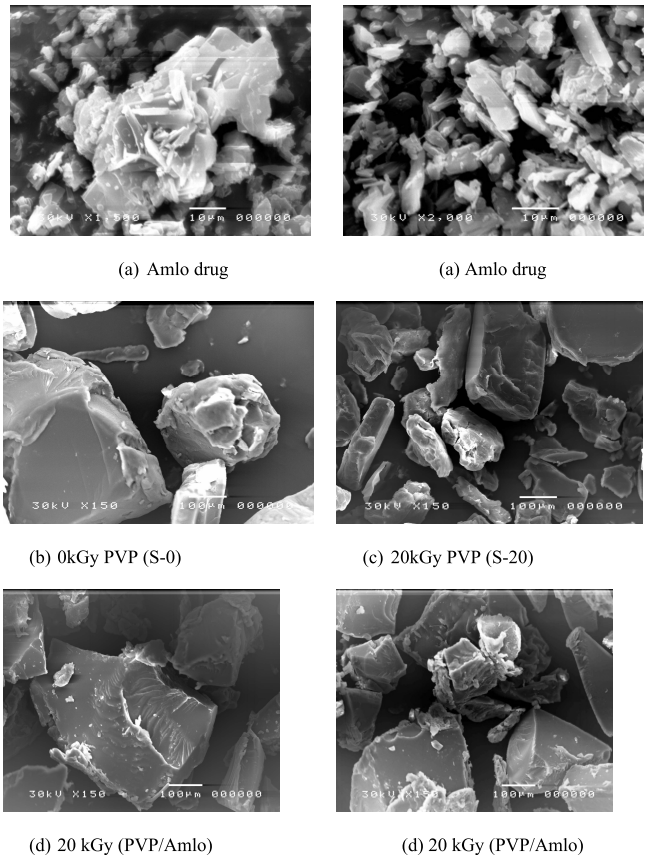

Figure 7. SEM micrographs for (PVP/Amlo) systems. (a) (Amlo) drug, (b) 0 kGy (PVP) (c) 20 kGy (PVP), and (d) 20 kGy (PVP/Amlo) at a 0.5:1 ratio.

abundance of amorphous structures in the unirradiated and moderately irradiated solid (PVP) samples.[60]

Table 4 summarizes the crystallite size (D, nm) that was measured using the Debye−Scherer formula as an estimate of grain size. It has been found that the D value of (PVP) samples decreased as the radiation dose increased, which indicates that the grain size expectedly decreased. The crystallite size of the native (PVP) sample was measured as 2.81 nm and decreased considerably after irradiation at 10, 20, 30, 40, and 50 kGy to reach 2.66, 2.21, 1.02, 0.90, and 0.88 nm, respectively. A lower crystallite size (D, nm) was observed at 50 kGy. The decrease in the crystallite size reached about 68.41% compared to the blank sample. It concluded that after irradiation, the (PVP) structure could be changed.

Figure 5c illustrates the XRD pattern (PVP/Amlo). It is clear from this figure that gamma rays induce a slight shift of the XRD peak (100%) at $2\theta \approx 11$ and 22° for the irradiated (PVP) samples. The relative intensities of $2\theta \approx 11^{\circ}$ decreased when the radiation dose increased, which indicates that the lattice plane of $2\theta \approx 11^{\circ}$ changed due to the interaction that occurred between (PVP) and (Amlo) molecules with the grain size expected to increase. This indicated that the (PVP) inhibited the recrystallization process of drug molecules and exhibited amorphous solid dispersions.

3.4. FT-IR of Gamma-Irradiated Solid (PVP) and (PVP/Amlo). Figure 6a shows FT-IR analysis of the (Amlo) solid forms. The characteristic O−H stretching band was absent in the FT-IR spectrum; this indicated that the (Amlo) is in AH form. In addition, the IR peak at 3293 cm^{-1} is attributed to the N−H stretching bond, which was characteristic to the AH form.[56] The two peaks located at 1668 and 1614 cm^{-1} possess two C═O groups from ethyl ester and methyl ester side chains, respectively. The infrared spectra of C═O of the (PVP/Amlo) are located at 1650 cm^{-1} as shown in Figure 6b. By means of shifting of C═O peaks of both drug and (PVP) molecules, individually, the intermolecular hydrogen bonds exist between the (PVP) and (Amlo) molecule group, which is the interface of the intramolecular hydrogen bonds that exist between the (Amlo−Amlo) molecule group (Figure 6a). The presence of hydrogen bonds between (Amlo) and the hydrophilic polymers (PVP) in the solid dispersions is the primary cause of the rise in its solubility and dissolution.[61,62]

3.5. Scanning Electron Microscopy (SEM). Figure 7a,b displays the crystallite and amorphous structures for the (Amlo) drug and native (PVP) powder, respectively. The crystals structure of the (Amlo) drug seemed to be irregular in size and shape. The grain size of the (Amlo) drug was smaller than native (PVP) powder. The irradiated (PVP) powder at a dose of 20 kGy (S-20) is shown in Figure 7c, it is clear from the SEM image that gamma rays reduced the size of native (PVP) particles. The decrease in native (PVP) grain size induced by gamma rays is

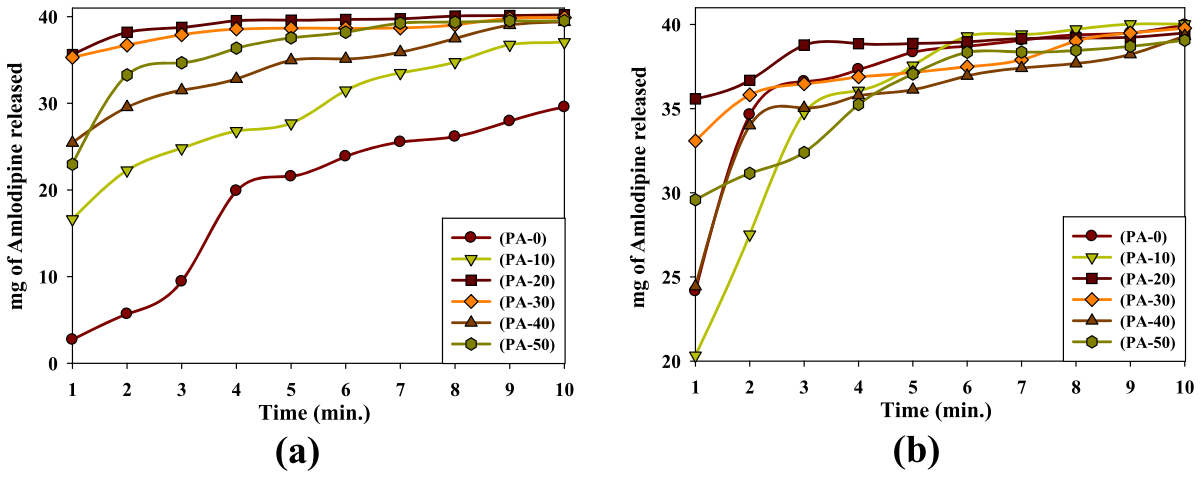

Figure 8. In vitro release profile of (Amlo−PVP) formulations prepared by solid dispersions for a 1:2 ratio of irradiated (PVP) at different doses (a) at pH 7 and (b) at pH 1.2.

https://dx.doi.org/10.1021/acsomega.0c01910
ACS Omega 2020, 5, 21476−21487

due to the lattice distortions in the native (PVP) structure. Figure 7d showed the amorphous structures of the physical mixture of the 20 kGy (PVP/Amlo) (PA-20). It was difficult to distinguish the presence of (Amlo) drug crystals due to (Amlo) crystals incorporated into the matrix of amorphous (PVP) particles. This result was in full agreement with the results of XRD.

3.6. In Vitro Dissolution Study Results. Figure 8a,b shows the released (Amlo) molecules with time at pH 7 and pH 1.2, respectively. As seen in Figure 8a, in all prepared (PVP/Amlo) samples, the dissolution rate increases drastically from (PA-0), (PA-10), (PA-40), (PA-50), (PA-30) to (PA-20). In Figure 8b, the release rate of (Amlo) significantly changed in the order of (PA-10), (PA-40), (PA-0), (PA-50), (PA-30), and (PA-20).

Analysis of the above results showed that the irradiated (PVP) powder leads to increasing release of the (Amlo) drug compared with the unirradiated sample. This is probably due to the higher intermolecular H bonds and amorphous structure of (Amlo/PVP). At pH 1.2, samples of (PA-0), (PA-10), (PA-20), (PA-30), (PA-40), and (PA-50) are released for 60.37, 50.82, 88.95, 82.70, 61.09, and 73.94% at the first minute, respectively. At pH 7, samples of (PA-0), (PA-10), (PA-20), (PA-30), (PA-40), and (PA-50) are released for 6.82, 41.57, 89.04, 88.25, 63.60, and 57.40% at the first minute, respectively. This indicated that the solubility of the (PA-20) sample is substantially enhanced compared to residual samples.

4. CONCLUSIONS

In this article, the changes in physicochemical properties of a (PVP) biocompatible material in powder form induced by gamma irradiation were investigated with the aim of evaluating their effect on enhancing the dissolution of the amlodipine drug. In particular, a set of six (PVP) samples were irradiated with varying gamma rays dose up to 50 kGy under a nitrogen atmosphere. X-ray diffraction techniques illustrated the amorphous nature of the (PVP) formulation under conditions of gamma irradiation. Further, the radiation impact on solid (PVP) was examined by FT-IR powered by ESR; these spectra indicate that the formation of new functional groups created on the developed segmental molecules were produced by the radiation-induced chain scission mechanism. The formation and shifting of the broad OH and C═O peaks by a dose determined the affordability of establishing an interpolymer interaction cross-linkage via hydrogen bonding among the radiation-induced opening of the (PVP) ring and the hyperfine splitting due to the radical interaction with proton at Cα and Cβ in a hollow (PVP) chain; in actuality, the gamma irradiation of the (PVP) solid could cause the opening of pyrrolidone ring. The irradiated (PVP) samples are used as a carrier of the (Amlo) drug to enhance their dissolution and bioavability. It is clear from the SEM image that gamma rays reduced the size of native (PVP) particles. The decrease in native (PVP) grain size induced by gamma rays is due to the lattice distortions in the native (PVP) structure. A higher dissolution rate of (Amlo) observed with irradiated (PVP) (compared to the blank (PVP) sample) solid dispersion is due to the presence of (Amlo) in amorphous when incorporated with (PVP). This indicated that the (PVP) inhibited the recrystallization process of drug molecules and exhibited amorphous solid dispersions. The amorphous form produces a faster dissolution rate. FT-IR confirmed that the interaction (hydrogen bonding) between (PVP) and amlodipine affected their drug solubility. The change of the chemical structure of irradiated (PVP) at 20 kGy (PA-0) could be the strongest drug−polymer H-bond interaction that provides high drug dissolution behavior.

AUTHOR INFORMATION

Corresponding Authors

Mohamed Mohamady Ghobashy − *Radiation Research of Polymer Chemistry Department, National Center for Radiation Research and Technology (NCRRT), Atomic Energy Authority, Cairo 11787, Egypt*; orcid.org/0000-0003-0968-1423; Email: Mohamed.ghobashy@eaea.org.eg, Mohamed_ghobashy@yahoo.com

Mohamed Madani − *Faculty of Science and Humanities - Jubail, Imam Abdulrahman Bin Faisal University, Jubail 35811, Saudi Arabia*; Email: mmadani@iau.edu.sa

Authors

Dalal Mohamed Alshangiti − *Faculty of Science and Humanities - Jubail, Imam Abdulrahman Bin Faisal University, Jubail 35811, Saudi Arabia*

Sheikha A. Alkhursani − *Faculty of Science and Humanities - Jubail, Imam Abdulrahman Bin Faisal University, Jubail 35811, Saudi Arabia*

Samera Ali Al-Gahtany − *Faculty of Science, University of Jeddah, Jeddah 23218, Saudi Arabia*

Fathiah Salem Shokr − *King Abdulaziz University, Faculty of Science &Arts, Department of Physics, Rabigh 25732, Saudi Arabia*

Complete contact information is available at: https://pubs.acs.org/10.1021/acsomega.0c01910

Notes

The authors declare no competing financial interest.

ACKNOWLEDGMENTS

M.G. thanks the Faculty of Science and Humanities - Jubail, Imam Abdulrahman Bin Faisal University and Faculty of Science, University of Jeddah, Jeddah, Saudi Arabia, and King Abdulaziz University, Faculty of Science &Arts, Department of Physics, Saudi Arabia. This study was partially performed in Radiation Research of Polymer Chemistry Department, National Center for Radiation Research and Technology (NCRRT), Atomic Energy Authority, P.O.Box.29, Nasr City, Cairo, Egypt.

REFERENCES

(1) Hu, J.; Johnston, K. P.; Williams, R. O., III Nanoparticle engineering processes for enhancing the dissolution rates of poorly water soluble drugs. *Drug Dev. Ind. Pharm.* **2004**, *30*, 233−245.

(2) Junyaprasert, V. B.; Morakul, B. Nanocrystals for enhancement of oral bioavailability of poorly water-soluble drugs. *Asian J. Pharm. Sci.* **2015**, *10*, 13−23.

(3) Vo, C. L.-N.; Park, C.; Lee, B.-J. Current trends and future perspectives of solid dispersions containing poorly water-soluble drugs. *Eur. J. Pharm. Biopharm.* **2013**, *85*, 799−813.

(4) Vasconcelos, T.; Sarmento, B.; Costa, P. Solid dispersions as strategy to improve oral bioavailability of poor water soluble drugs. *Drug Discovery Today* **2007**, *12*, 1068−1075.

(5) Tiwari, R.; Tiwari, G.; Srivastava, B.; Rai, A. K. Solid dispersions: an overview to modify bioavailability of poorly water soluble drugs. *Int. J. PharmTech Res.* **2009**, *1*, 1338−1349.

(6) Chiou, W. L.; Riegelman, S. Preparation and dissolution characteristics of several fast-release solid dispersions of griseofulvin. *J. Pharm. Sci.* **1969**, *58*, 1505−1510.

https://dx.doi.org/10.1021/acsomega.0c01910
ACS Omega 2020, 5, 21476−21487

(7) Pokharkar, V. B.; Mandpe, L. P.; Padamwar, M. N.; Ambike, A. A.; Mahadik, K. R.; Paradkar, A. Development, characterization and stabilization of amorphous form of a low T_g *drug*. *Powder Technol.* **2006**, *167*, 20−25.
(8) Karagianni, A.; Kachrimanis, K.; Nikolakakis, I. Co-amorphous solid dispersions for solubility and absorption improvement of drugs: Composition, preparation, characterization and formulations for oral delivery. *Pharmaceutics* **2018**, *10*, 98.
(9) Ghobashy, M. M.; Elhady, M. A. pH-sensitive wax emulsion copolymerization with acrylamide hydrogel using gamma irradiation for dye removal. *Radiat. Phys. Chem.* **2017**, *134*, 47−55.
(10) Ghobashy, M. M. Combined ultrasonic and gamma-irradiation to prepare TiO_2@PET-g-PAAc fabric composite for self-cleaning application. *Ultrason. Sonochem.* **2017**, *37*, 529−535.
(11) Sinha, D.; Sahoo, K. L.; Sinha, U. B.; Swu, T.; Chemseddine, A.; Fink, D. Gamma-induced modifications of polycarbonate polymer. *Radiat. Eff. Defects Solids* **2004**, *159*, 587−595.
(12) Alwan, T. J. Gamma irradiation effect on the optical properties and refractive index dispersion of dye doped polystyrene films. *Turk. J. Phys.* **2012**, *36*, 377−384.
(13) Zaki, M. F. Gamma-induced modification on optical band gap of CR-39 SSNTD. *Braz. J. Phys.* **2008**, *38*, 558−562.
(14) Fehérvári, A.; Földes-Berezsnich, T.; Tüdös, F. Kinetics of Radical Polymerization. XXIX. Kinetics of Initiation in the Polymerization of Ethyl Acrylate. *J. Macromol. Sci. Chem.* **2006**, *14*, 1071−1084.
(15) Ghobashy, M. M. Ionizing radiation-induced polymerization. In *Ionizing Radiation Effects and Applications*; 2018, PP 113, DOI: 10.5772/intechopen.73234.
(16) Haugen, H. J.; Brunner, M.; Pellkofer, F.; Aigner, J.; Will, J.; Wintermantel, E. Effect of different γ-irradiation doses on cytotoxicity and material properties of porous polyether-urethane polymer. *J. Biomed. Mater. Res., Part B* **2006**, *80B*, 415−423.
(17) Raghu, S.; Archana, K.; Sharanappa, C.; Ganesh, S.; Devendrappa, H. The physical and chemical properties of gamma ray irradiated polymer electrolyte films. *J. Non-Cryst. Solids* **2015**, *426*, 55−62.
(18) Singh, S.; Singh, N.; Ezekiel, R.; Kaur, A. Effects of gamma-irradiation on the morphological, structural, thermal and rheological properties of potato starches. *Carbohydr. Polym.* **2011**, *83*, 1521−1528.
(19) McKellop, H. A. *Does Gamma Radiation Speed or Slow Wear*; Bulletin, The American Academy of Orthopedic Surgeons, 1996, 44.
(20) Ortega, A.; Bucio, E.; Burillo, G. Radiation polymerization and crosslinking of (N-isopropylacrylamide) in solution and in solid state. *Polym. Bull.* **2007**, *58*, 565−573.
(21) Nagaoka, N.; Safrani, A.; Yoshida, M.; Omichi, H.; Kubota, H.; Katakai, R. Synthesis of poly(N-isopropylacrylamide) hydrogels by radiation polymerization and crosslinking. *Macromolecules* **1993**, *26*, 7386−7388.
(22) Qin, C. Q.; Du, Y. M.; Xiao, L. Effect of hydrogen peroxide treatment on the molecular weight and structure of chitosan. *Polym. Degrad. Stab.* **2002**, *76*, 211−218.
(23) Pérez Perrino, M.; Navarro, R.; Gómez Tardajos, M.; Gallardo, A.; Reinecke, H. "One-pot" Synthesis of 1-Vinyl-2-pyrrolidone with Protic Functional Groups in 3-Position. *Macromol. Chem. Phys.* **2009**, *210*, 1973−1978.
(24) Dorati, R.; Colonna, C.; Serra, M.; Genta, I.; Modena, T.; Pavanetto, F.; Perugini, P.; Conti, B. γ-Irradiation of PEGd, lPLA and PEG-PLGA multiblock copolymers: I. effect of irradiation doses. *AAPS PharmSciTech* **2008**, *9*, 718−725.
(25) Jellinek, H. H. G.; Wang, L. C. The Photolysis of Polyvinylpyrrolidone in Aqueous Solutions in the Presence of Oxygen and Cupric Ions. *J. Macromol. Sci. Chem.* **1968**, *2*, 1353−1367.
(26) Yousif, E.; Haddad, R. Photodegradation and photostabilization of polymers, especially polystyrene: review. *SpringerPlus* **2013**, *2*, 398.
(27) Mazumdar, N. A.; Vardarajan, R.; Singh, H. Iodine-incorporated copolymer of methyl methacrylate and N-vinylpyrrolidone. I. Synthesis and characterization. *J. Macromol. Sci., Part A: Pure Appl. Chem.* **1996**, *33*, 353−370.
(28) Yu, J.; Shi, Y.; Zhao, K.; Yang, G.; Yu, L.; Li, Y.; Andersson, E.-M.; Ämmälä, C.; Yang, S.-N.; Berggren, P.-O. Enhanced expression of β cell CaV3. 1 channels impairs insulin release and glucose homeostasis. *Proc. Natl. Acad. Sci. U. S. A.* **2020**, *117*, 448−453.
(29) Dahima, R.; Pachori, A.; Netam, S. Formulation and evaluation of mouth dissolving tablet containing amlodipine besylate solid dispersion. *Int. J. ChemTech Res.* **2010**, *2*, 706−715.
(30) Jaya, S.; Amala, V. Formulation and In-vitroEvaluation of Oral Disintegrating Tablets of Amlodipine Besylate. *Int. J. Adv. Pharm.* **2019**, *11*, 49−54.
(31) Sabar, M. H. Formulation and in vitro evaluation of fast dissolving film containing amlodipine besylate solid dispersion. *Int. J. Pharm. Pharm. Sci.* **2013**, *5*, 419−428.
(32) Kamagoni, K.; Gunnala, P. G.; Somagoni, J. Preparation and enhancement of dissolution rate of amlodipine besylate and valsartan using liquisolid technique. *Pharm. Globale* **2013**, *4*, 1.
(33) Tyagi, V. K.; Singh, D.; Pathak, K. Semisolid matrix-filled hard gelatin capsules for rapid dissolution of amlodipine besilate: Development and assessment. *J. Adv. PharmTech Res.* **2013**, *4*, 42−49.
(34) Ayorinde, J. O.; Odeniyi, M. A.; Balogun-Agbaje, O. Formulation and Evaluation of Oral Dissolving Films of amlodipine besylate using blends of starches with hydroxypropyl methyl cellulose. *Polim. Med.* **2016**, *46*, 45−51.
(35) Jang, D.-J.; Sim, T.; Oh, E. Formulation and optimization of spray-dried amlodipine solid dispersion for enhanced oral absorption. *Drug Dev. Ind. Pharm.* **2013**, *39*, 1133−1141.
(36) Pare, A.; Yadav, S. K.; Patil, U. K. Formulation and evaluation of effervescent floating tablet of amlodipine besylate. *Res. J. Pharm. Technol.* **2008**, *1*, 526−530.
(37) Shelke, P. V.; Dumbare, A. S.; Gadhave, M. V.; Jadhav, S. L.; Sonawane, A. A.; Gaikwad, D. D. Formulation and evaluation of rapidly dis integrating film of amlodipine bes ylate. *J. Drug Delivery Ther.* **2012**, *2*, DOI: 10.22270/jddt.v2i2.85.
(38) O'donnell, J. H.; Rahman, N. P.; Smith, C. A.; Winzor, D. J. Chain scission and cross-linking in the radiation degradation of polymers: limitations on the utilization of theoretical expressions and experimental results in the Pregel region. *Macromolecules* **1979**, *12*, 113−119.
(39) Zhang, X. C.; Butler, M. F.; Cameron, R. E. The ductile−brittle transition of irradiated isotactic polypropylene studied using simultaneous small angle X-ray scattering and tensile deformation. *Polymer* **2000**, *41*, 3797−3807.
(40) Loo, S. C. J.; Ooi, C. P.; Boey, Y. C. F. Radiation effects on poly(lactide-co-glycolide)(PLGA) and poly(L-lactide)(PLLA). *Polym. Degrad. Stab.* **2004**, *83*, 259−265.
(41) Charlesby, A. *Atomic radiation and polymers*; Elsevier: 2016.
(42) Saito, O. On the effect of high energy radiation to polymers. I. cross-linking and degradation. *J. Phys. Soc. Jpn.* **1958**, *13*, 198−206.
(43) Gilding, D. K.; Reed, A. M. Biodegradable polymers for use in surgery-polyglycolic/poly(actic acid) homo- and copolymers: 1. *Polymer* **1979**, *20*, 1459−1464.
(44) Hausberger, A. G.; Kenley, R. A.; DeLuca, P. P. Gamma irradiation effects on molecular weight and in vitro degradation of Poly(D,L-lactide-CO-glycolide) microparticles. *Pharm. Res.* **1995**, *12*, 851−856.
(45) Devries, K. L.; Igarashi, M.; Chao, F. Molecular degradation of polymers. In *Journal of Polymer Science: Polymer Symposia*; Wiley Subscription Services, Inc.: New York, 1985, *72*, 111−129.
(46) Buchachenko, A. L. Complexes of Molecular Oxygen with Organic Molecules. *Russ. Chem. Rev.* **1985**, *54*, 117.
(47) Mustafi, D.; Makinen, M. W. Application of angle-selected electron nuclear double resonance to characterize structured solvent in small molecules and macromolecules. In *Biomedical EPR, Part B: Methodology, Instrumentation, and Dynamics*; Springer: Boston, MA, 2005, 89−144.
(48) Mönig, H.; Ringsdorf, H. ESR investigations of γ-irradiated sulfur-containing vinylpolymers. *Makromol. Chem.* **1974**, *175*, 811−822.

https://dx.doi.org/10.1021/acsomega.0c01910
ACS Omega 2020, 5, 21476−21487

(49) Bamford, C. H.; Ward, J. C. Radical oxidation studied by electron resonance. *Trans. Faraday Soc.* **1962**, *58*, 971−981.
(50) Szöcs, F.; Hloušková, Z.; Tiňo, J. E.s.r. study of free radicals in poly(vinyl carbazole). *Polymer* **1980**, *21*, 1062−1064.
(51) Zott, H.; Heusinger, H. Intermediates of radiation-induced polymerisation of maleimides studied by ESR. *Eur. Polym. J.* **1978**, *14*, 89−92.
(52) Erizal, E.; Tjahyono, T.; Dian, P. P.; Darmawan, D. Synthesis of Polyvinyl Pirrolidone (PVC)/K-Carrageenan Hydrogel Prepared by Gamma Radiation Processing As a Function of Dose and PVP Concentration. *Ind. J. Chem.* **2013**, *13*, 41−46.
(53) Khanna, P. K.; Gokhale, R.; Subbarao, V. V. V. S. Poly (vinyl pyrolidone) coated silver nano powder via displacement reaction. *J. Mater. Sci.* **2004**, *39*, 3773−3776.
(54) Hassouna, F.; Therias, S.; Mailhot, G.; Gardette, J. L. Photooxidation of poly (N-vinylpyrrolidone)(PVP) in the solid state and in aqueous solution. *Polym. Degrad. Stab.* **2009**, *94*, 2257−2266.
(55) Zhang, Y.; Hu, W.; Li, B.; Peng, C.; Fan, C.; Huang, Q. Synthesis of polymer-protected graphene by solvent-assisted thermal reduction process. *Nanotechnology* **2011**, *22*, 345601.
(56) Koradia, V.; de Diego, H. L.; Frydenvang, K.; Ringkjøbing-Elema, M.; Müllertz, A.; Bond, A. D.; Rantanen, J. Solid forms of amlodipine besylate: physicochemical, structural, and thermodynamic characterization. *Cryst. Growth Des.* **2010**, *10*, 5279−5290.
(57) Alex, A.; Millan, D. S.; Perez, M.; Wakenhut, F.; Whitlock, G. A. Intramolecular hydrogen bonding to improve membrane permeability and absorption in beyond rule of five chemical space. *Med. Chem. Commun* **2011**, *2*, 669−674.
(58) Woolfson, A. D.; McCafferty, D. F.; Launchbury, A. P. Stabilisation of hydrotropic temazepam parenteral formulations by lyophilisation. *Int. J. Pharm.* **1986**, *34*, 17−22.
(59) Saluja, H.; Mehanna, A.; Panicucci, R.; Atef, E. Hydrogen bonding: Between strengthening the crystal packing and improving solubility of three haloperidol derivatives. *Molecules* **2016**, *21*, 719.
(60) Zheng, M.; Gu, M.; Jin, Y.; Jin, G. Optical properties of silver-dispersed PVP thin film. *Mater. Res. Bull.* **2001**, *36*, 853−859.
(61) Hutchins, K. M. Functional materials based on molecules with hydrogen-bonding ability: applications to drug co-crystals and polymer complexes. *R. Soc. Open Sci.* **2018**, *5*, 180564.
(62) Wlodarski, K.; Sawicki, W.; Haber, K.; Knapik, J.; Wojnarowska, Z.; Paluch, M.; Lepek, P.; Hawelek, L.; Tajber, L. Physicochemical properties of tadalafil solid dispersions−Impact of polymer on the apparent solubility and dissolution rate of tadalafil. *Eur. J. Pharm. Biopharm.* **2015**, *94*, 106−115.

https://dx.doi.org/10.1021/acsomega.0c01910
ACS Omega 2020, 5, 21476−21487